

Preliminary Magnetic Field Optimization of HGQS05 End Regions

G. Sabbi

1 Introduction

The HGQ coil end optimization is proceeding according to the guidelines defined by the HGQ short model program [1].

The first design iteration, which was adopted for model HGQS01, consisted of a magnetic analysis and optimization of the position of the conductor groups in the return end [2], followed by a detailed mechanical design of both the return and the lead end parts [3].

In the HGQS02 model, the second-wound conductor group in the outer coil was shifted outwards by 2 cm with respect to its previous position. This decision was taken after a new magnetic analysis of the baseline design showed that the peak field in the HGQS01 outer coil end is higher than previously indicated and limits the magnet performance [4, 5]. The modified geometry allows to reduce the peak field with minor modification of the end parts. A magnetic analysis of the HGQS02 end configuration is reported in [6].

The main new feature of the HGQS03 is the design of the joint connecting the inner and outer coil in the lead end of each quadrant. HGQS01 and HGQS02 feature an external splice placed outside the radial boundary of the coil, therefore requiring the use of special end collets for mechanical support. HGQS03 features an internal splice entirely contained within the radial boundary of the coil [7]. The goal is to provide better mechanical support and to simplify magnet assembly by replacing the end collets with collars over the whole length. A magnetic field analysis of the HGQS03 lead end is reported in [8]. The return end configuration in HGQS03 is identical to that of HGQS02.

The coil end optimization of HGQS04 focuses on mechanical issues. The goal is to reduce the mechanical length from the coil termination to the outer surface of the end plate by about 4 cm on each side, and to improve the quadrant splice design. Although the corresponding variation in the length of the main leads impacts the field quality, this variation can be compensated by properly shifting the conductor groups in the lead end.

The short model program calls for the final HGQ end configuration to be reached in magnet HGQS05. Although some open issues (internal vs external splice, end plate thickness) do not allow to finalize the design at this stage, a preliminary study was carried out to evaluate the cost and benefits of different optimization strategies from the point of view of magnetic vs physical length ratio, operating margin to quench, and field quality.

2 Computer Model

The magnetic field analysis and optimization has been performed using ROXIE [9]. The field calculation is based on the Biot-Savart law. The iron yoke is regarded as a magnetic mirror of circular shape (inner radius 9.256 cm) with infinite permeability. The lead and the return end calculations are performed independently. For each case, a straight section extending for 1.5 m inwards from the start of the iron yoke is included in the model. Since many different configurations have to be evaluated in the optimization process, in order to reduce the computation time a simplified model has been adopted with respect to previous studies [4, 6, 8]: instead than using a current filament for each strand, each conductor has been subdivided in 10 current filaments along its width; the width of the interval over which the integrated multipoles are computed has been reduced by 10 cm in the lead end and 15 cm in the return end; the field integration step used was 2 mm instead than 1 mm. The error introduced by these simplifications was studied by recalculating some of the existing end configurations. It was found that the accuracy is adequate for a preliminary optimization study. Moreover, this error is comparable to the uncertainty related to the mechanical optimization still in progress, and to the observed differences between calculated and measured harmonics [10], which are primarily due to fabrication tolerances. The quadrant splice geometry is not included in the model. However, both theoretical considerations and the comparison between calculated and measured harmonics in HGQS01 show that the effect is small [10]. The final optimization will be performed using a more refined model and incorporating the results of the mechanical optimization.

3 Field quality representation

The field quality in the end regions will be expressed in terms of integrated multipole components, defined according to the following expression:

$$\int_{z_p}^{z_q} [B_y(x, y, z) + iB_x(x, y, z)]dz = \sum_{n=1}^{\infty} (\hat{B}_n^{[z_p, z_q]} + i\hat{A}_n^{[z_p, z_q]}) \left(\frac{x + iy}{r_0} \right)^{n-1} \quad (1)$$

This expansion is only valid if the integration interval covers the whole end region, i.e. if the starting point z_p is sufficiently inside the magnet body and the end point z_q is sufficiently far away from the coil termination. With the coordinate system defined in [3], the integration range is [-25,+20] cm in the lead end and [-10, +15] cm in the return end.

It is often convenient to express the integrated multipole components \hat{B}_n , \hat{A}_n in the end regions in “units” of 10^{-4} of the main integrated quadrupole field $\hat{B}_2^{[z_p, z_q]}$:

$$\hat{b}_n^{[z_p, z_q]} = \frac{\hat{B}_n^{[z_p, z_q]}}{\hat{B}_2^{[z_p, z_q]}} \cdot 10^4 \quad (2)$$

$$\hat{a}_n^{[z_p, z_q]} = \frac{\hat{A}_n^{[z_p, z_q]}}{\hat{B}_2^{[z_p, z_q]}} \cdot 10^4 \quad (3)$$

The magnetic length L_m of the interval $[z_p, z_q]$ is defined as the length which would provide an equivalent integrated quadrupole field in the magnet body:

$$L_m^{[z_p, z_q]} = \hat{B}_2^{[z_p, z_q]} / B_2 \quad (4)$$

B_2 is the quadrupole field component in the straight section. The magnetic length calculation is based on a transfer function in the magnet body of 0.1822 T/m/kA, as obtained for a 2D analysis carried out under the same assumptions (conductors aligned to the coil outer radius, circular iron yoke of inner radius 9.2564 cm and infinite permeability) [11].

In order to analyze the contributions to the integrated harmonic components from different parts of the coil end, and to compare different configurations, it is convenient to split the integration in a sequence of short consecutive intervals along z : $[z_i, z_{i+1}]$, $i = 1, N$, with $z_i = z_p + (i - 1)\Delta$, $\Delta = (z_q - z_p)/N$. For this purpose, the integrated multipole components are most conveniently expressed in terms of “units” of 10^{-4} of the integral of the main quadrupole field B_2 *in the straight section* extended over the same physical length:

$$\bar{b}_n^{[z_i, z_{i+1}]} = \frac{1}{B_2 \Delta} \hat{B}_n^{[z_i, z_{i+1}]} \cdot 10^4 \quad (5)$$

$$\bar{a}_n^{[z_i, z_{i+1}]} = \frac{1}{B_2 \Delta} \hat{A}_n^{[z_i, z_{i+1}]} \cdot 10^4 \quad (6)$$

It should be noted that since the intervals $[z_i, z_{i+1}]$ do not in general satisfy the requirement of vanishing longitudinal field at their boundaries, the Fourier expansion 1 for the $\hat{B}_n^{[z_i, z_{i+1}]}$ components is only valid at the radius r_0 .

All harmonics are given at a reference radius $r_0=17$ mm [12].

4 Mechanical constraints

The following mechanical constraints have to be taken into account:

- In order to simplify assembly and provide better mechanical support, the number of conductor groups has to be kept as small as possible. The minimum is given by the number of current blocks in the straight section (4). Although solutions with 5 blocks have been considered for both the lead and the return end, a 4-block configuration is strongly preferred.
- In order to prevent the cable from collapsing during winding, the geometry of the groups must be such to minimize the strain energy in each conductor; for this reason, the BEND-optimized geometries of the HGQS01-3 groups have been preserved whenever possible, and only the origin differences of the groups have been used as optimization variables.
- the spacers must be sufficiently thick to avoid breakage in high stress points, and provisions for features required for magnet assembly and mechanical support have to be included. A

minimum thickness at the pole of 13 mm has been required for spacers. The origin shift of the second-wound conductor group of the outer layer has not been decreased in order to maintain the wedge transition cut-out. The start of the coil to coil splice ramp in the inner layer has been kept at a constant distance relative to the first-wound conductor group in the outer layer, in order to avoid any interference. Some of these choices are rather conservative and may be slightly relaxed in the final optimization.

5 Optimization objectives

The coil end optimization objectives are to achieve a high ratio of magnetic vs physical length, to minimize the peak field in the coil and to minimize the integrated harmonics. These objectives are in conflict with each other: for example, in order to improve the magnetic vs. physical length ratio, the coil has to be made more compact, causing an increase of the peak field and reducing the degrees of freedom for field quality optimization. In order to better understand the design space for each of the objectives, they will be first reviewed separately.

5.1 Magnetic length

The return end configurations of the first three HGQ models have been compared with the following cases (Fig. 1):

1. Truncated end. In this case the coil is truncated at the end of the straight section. This is of course unphysical, but shows what is the best possible ratio of magnetic vs. physical length.
2. Compact end. In this case, a very short path length has been chosen for the conductors, completely disregarding issues of cable mechanical stability and field quality. This result corresponds to giving the highest priority to the magnetic vs. physical length optimization.

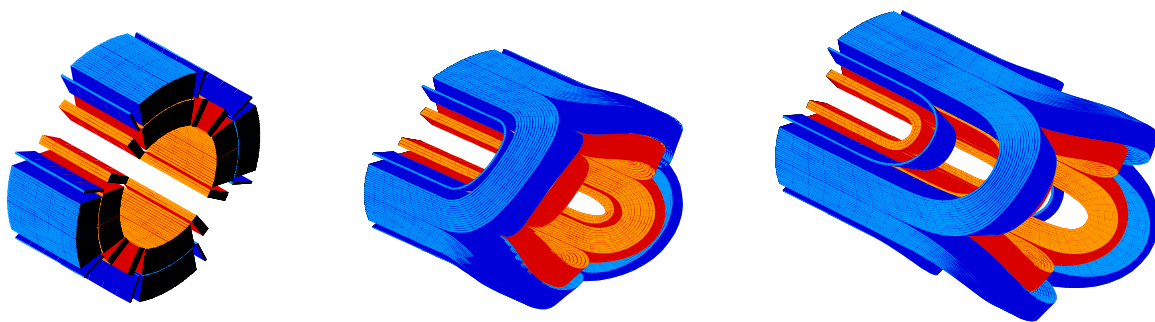


Figure 1: Left: truncated end; Center: compact end; Right: HGQS02-3 return end. Only the part of the coil extending beyond the edge of the iron yoke is shown; a 1.5 m straight section is also included in the model.

The physical length from a starting point z_s located 5 cm inwards with respect to the start of the iron yoke to the outmost conductor, and the magnetic length from the same point to $+\infty$

for each case are shown. In the truncated end case, the physical and magnetic length are almost equivalent. However, in any realistic configuration, at least 2.4 cm of magnetic length are lost with respect to the coil physical length. The design range for the parameter L_p-L_m in the HGQ is therefore $\approx [2.4, 4]$ cm. The corresponding lead end parameters for HGQS01-3 are shown in Table 2.

Table 1: Magnetic vs. physical length comparison (return end). L_p is the physical distance from the starting point $z_s=-10$ cm (5 cm before the iron yoke termination) to the outer edge of the outmost conductor group. L_m is the magnetic length from z_s to $+\infty$.

Parameter	Unit	HGQS03/HGQS02	HGQS01	Truncated	Compact
L_p	cm	21.65	20.67	10	14.8
L_m	cm	17.50	16.78	9.7	12.4
$L_p - L_m$	cm	4.15	3.89	0.3	2.4

Table 2: Magnetic vs. physical length comparison for the lead end configurations of the first three HGQ models. L_p is the physical distance from the starting point $z_s=-25$ cm (10 cm before the iron yoke termination) to the outer edge of the outmost conductor group (without considering the lead conductors). L_m is the magnetic length from z_s to $+\infty$.

Parameter	Unit	HGQS03	HGQS02	HGQS01
L_p	cm	36.50	36.50	35.48
L_m	cm	31.54	31.39	30.72
$L_p - L_m$	cm	4.96	5.11	4.76

Table 3: Peak field (T/kA) in the first three HGQ models.

Layer	Lead end			Return end		Body (I=14 kA)
	HGQS03	HGQS02	HGQS01	HGQS03/HGQS02	HGQS01	
Inner	0.639	0.639	0.639	0.654	0.656	0.687
Outer	0.571	0.571	0.576	0.573	0.599	0.576

5.2 Peak field

Due to the complicated geometry of the conductors in the end regions, the coil windings cannot be clamped as tightly as in the straight section, and are thus more vulnerable to motion induced by Lorentz forces (both transverse and longitudinal). For this reason, it is desirable to increase the operating margin in the coil ends with respect to the magnet body. On the other hand, due to the (3D) current concentration, a local field enhancement of about 10% is usually observed in the coil head. This effect is compensated by removing the iron yoke in the end regions, which allows a peak field reduction of 10-20%. In the case of the HGQ, however, since the yoke contribution to

the peak field is less than 10%, it is important to obtain additional margin by careful design of the spacers, so that the highest field point moves away from the coil heads into the straight section, where the conductors are firmly confined by the collars.

The peak field parameters for the lead and return end, and for the straight section of the first three HGQ models, are shown in Table 3. As can be seen, in the case of HGQS01 the peak field in the outer layer of the return end is higher than in the magnet body, and limits the short sample performance of the magnet even if perfect mechanical support is assumed.

The relative position of the conductor groups at the pole plane for HGQS01 and HGQS02 is shown in Fig. 2. Fig. 3 (left) shows the magnetic field along z in the return end of HGQS01 and HGQS02. The high peak field in HGQS01 is due to a constructive interference of the contributions of block 1 (outer layer) and block 3 (inner layer). By shifting block 1 outwards by 2 cm in HGQS02, this situation has been corrected. In the lead end, some additional margin is obtained because due to the presence of the current leads, both of the second wound groups in the inner and outer layer have one less conductor than in the return end. The goal for the HGQS05 end optimization is to obtain a peak field equal or lower with respect to HGQS02.

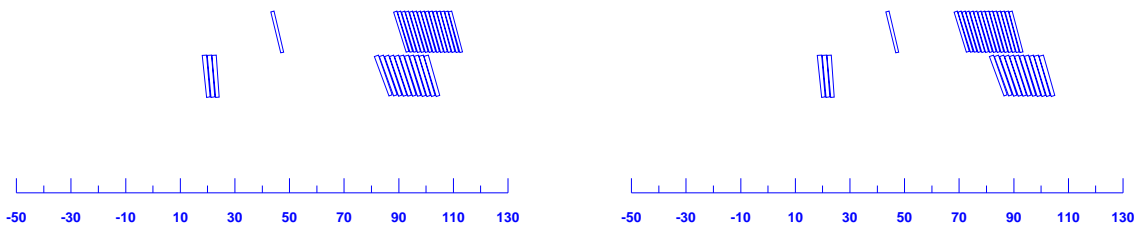


Figure 2: Longitudinal section at the pole angle for the return end of HGQS02 (left) and HGQS01 (right). Axis scale is in mm.

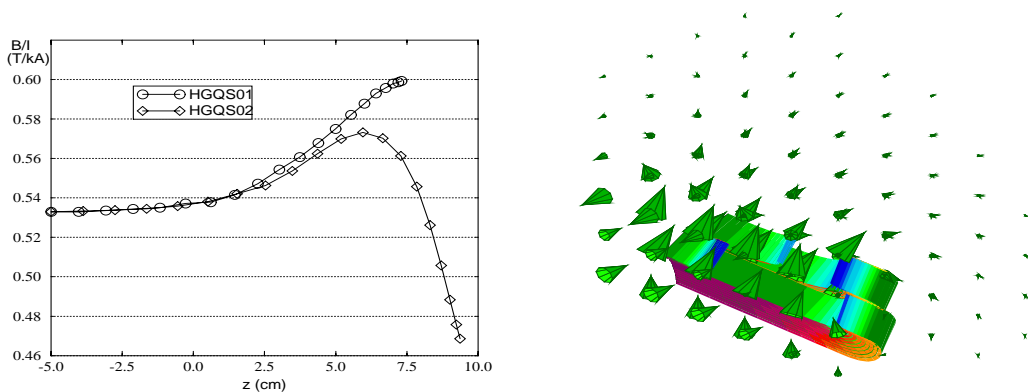


Figure 3: Left: field load line as function of z for the peak field conductor in the outer layer of HGQS01 and HGQS02 [4]. Right: magnetic field plot for HGQS01 showing the peak field enhancement resulting from the constructive interference of the contributions of block 1 and 3.

5.3 Field Quality

Table 4 shows the calculated systematic harmonics in the lead and return end of the first three HGQ models, and the expected systematic and random harmonics in the HGQ straight section. The expected quadrupole error in the straight section has not been studied in detail. The value in Table 4 is based on 1 mrad alignment accuracy (both systematic and random). As can be seen in the second part of the table, when the difference in magnetic length is taken into account most of the end harmonics are small with respect to their straight section counterparts. The only component for which a further optimization is desirable is the normal dodecapole \hat{b}_6 .

Table 4: Field quality in the lead and return end of the first three HGQ models, and expected harmonics in the HGQ straight section. L_m is the magnetic length from the integration starting point z_s to $+\infty$. In the lead end, $z_s=-25$ cm (10 cm before the iron yoke termination). In the return end, $z_s=-10$ cm (5 cm before the iron yoke termination). The integrated harmonics are expressed in a 2D-like representation, averaged over L_m , and relative to a main quadrupole component $\hat{b}_2=10000$.

Param	Lead end			Return end		Straight section	
	S03	S02	S01	S03/02	S01	System. (\pm)	Random
L_m (m)	0.315	0.314	0.307	0.175	0.168	5.0-5.8	
\hat{b}_6	6.57	7.26	6.60	2.3	0.87	0.2	0.3
\hat{b}_{10}	-0.30	-0.29	-0.29	-0.52	-0.53	0.1	0.1
\hat{a}_2	57.7	50.8	56.7			20	20
\hat{a}_6	-0.45	0.22	0.28			0.2	0.3
\hat{a}_{10}	-0.055	-0.097	-0.097			0.1	0.1
$\hat{b}_6 L_m$ (m)	2.07	2.28	2.03	0.40	0.15	1.0	1.6
$\hat{b}_{10} L_m$ (m)	-0.09	-0.09	-0.09	-0.09	-0.09	0.5	0.5
$\hat{a}_2 L_m$ (m)	18.2	15.9	17.4			110	110
$\hat{a}_6 L_m$ (m)	-0.14	0.07	0.09			1.0	1.6
$\hat{a}_{10} L_m$ (m)	-0.02	-0.03	-0.03			0.5	0.5

In the magnet straight section, the contribution to the normal dodecapole from eight line current located at quadrupole-symmetric locations with respect to a line current I_1 located at $r=a$, $\theta=\phi$ in the first quadrant is given by:

$$B_6 = -\frac{4\mu_0}{\pi a} \left(\frac{r}{a}\right)^5 I_1 \cos(6\phi) \quad (7)$$

When $I_1 < 0$ (as required in order to obtain $B_2 > 0$) the contribution to B_6 is positive and maximum for $\phi=0$, it decreases to zero in the interval $0 < \phi < \pi/12$, then it becomes negative, reaching a negative maximum for $\phi = \pi/6$, then it again decreases to zero in the interval $\pi/6 < \phi < \pi/4$. In the magnet cross section, the position of the conductors is optimized so that the total dodecapole is almost zero. In the magnet ends, as the conductor paths are bent towards the pole, a large

negative dodecapole field should be expected. However, by separating longitudinally the return sections for different groups of conductors it is possible to obtain a bipolar dodecapole field, which again integrates to zero. This is shown in Fig. 4 for the case of the HGQS01 return end: due to the term $(r/a)^5$ in equation 7, $\bar{b}_6(z)$ is dominated by the contribution from the inner coil. A first positive contribution is obtained for $z \in [0, 2.3]$ cm, when the 3 conductors of the first wound group ramp from $\phi \approx \pi/6$ to $\phi \approx \pi/4$. An additional positive contribution is obtained for $z \in [2.3, 4.6]$ cm as the positive contribution from the second-wound group (which has an origin shift of 4.6 cm) is no more balanced by the contribution from the first-wound group. Finally, a large negative contribution is obtained when the conductors of the second-wound group are bent towards the pole.

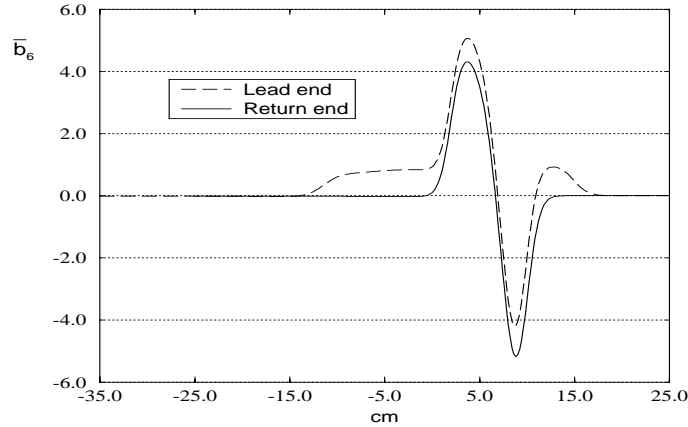


Figure 4: $\bar{b}_6(z)$ in the HGQS01 lead and return end [4].

In the lead end, both the leads ramping away from the pole region towards the coil to coil splice and the leads extending along the midplane towards the quadrant splice give additional positive contributions (Fig. 4). In this case, the origin shift of the second-wound group must be reduced with respect to the return end in order to obtain a small integrated dodecapole. This results in a more compact configuration with a better ratio of magnetic vs. physical length, although it may also cause an increase of the peak field.

6 Return End Optimization

The four current blocks of the reference octant in the HGQ cross section are labelled as follows: block 1 (15 conductors) for outer layer, midplane side; block 2 (1 conductor) for outer layer, pole side; block 3 (11 conductors) for inner layer, mid-plane side; block 4 (3 conductors) for inner layer, pole side. In order to preserve the wedge transition cut-out in the outer layer, which improves the mechanical structure and helps in preventing shorts, the 20 mm origin shift of block 1 has been preserved. This decision affects the total length of the end keys, but it does not cause any restrictions in the optimization, which focuses on the relative positions of the conductor groups.

Several configurations have been analyzed; the three most significant cases are discussed:

- REOPT1 is a 4-block configuration aiming at improving the magnetic vs. physical length

ratio. For this purpose, the origin shift of block 2, 3, 4, have been increased with respect to HGQS02/3. Although the position where the iron yoke is terminated will be optimized at a later stage in the program, to allow a consistent comparison the relative position of the iron yoke with respect to the closest conductor group (block 4 in this case) has been kept constant. The resulting geometry is shown in Fig. 5. The corresponding origin differences for each block are given in Table 5.

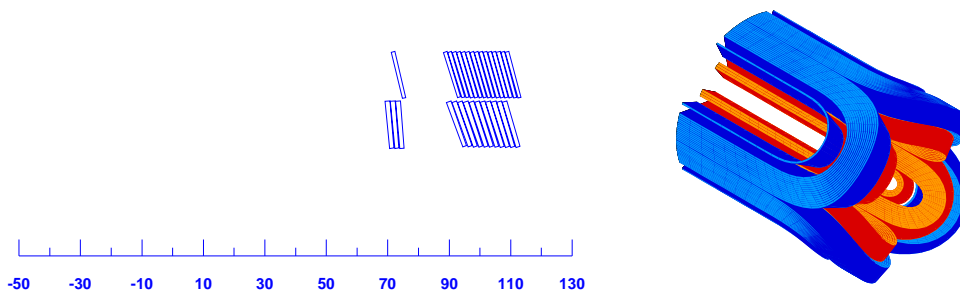


Figure 5: REOPT1 geometry. Axis scale for pole section is in mm.

- REOPT2 takes advantage of the additional degree of freedom obtained by splitting block 3 to improve significantly both the field quality and the magnetic length. This is obtained by introducing an additional origin shift for the conductors of block 3 located closest to the midplane (which give a large positive contribution to \hat{b}_6). In this way, a much shorter origin shift is sufficient to balance the integral as compared with what is required when block 3 is not split. However, since the new conductor groups resulting from splitting block 3 have not been optimized mechanically, the feasibility of this geometry has not been assessed yet. It should also be noted that the introduction of an additional spacer causes a loss of about 13 mm in compaction. The resulting geometry is shown in Fig. 6. The corresponding origin differences for each block are given in Table 5.

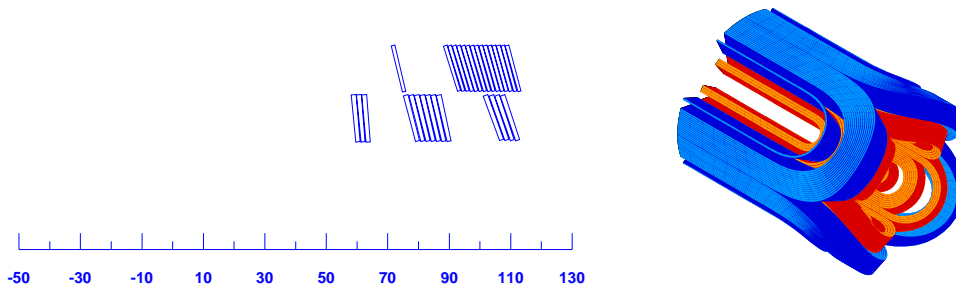


Figure 6: REOPT2 geometry. Axis scale for pole section is in mm.

- REOPT3 is a 4-block solution which allows small improvements of all parameters (magnetic length, peak field, field quality) with respect to HGQS02-3. The integrated normal dodecapole is positive in HGQS02-3. A negative contribution is created by reducing the separation

between the return sections of block 3-4. In order to increase the magnetic length, it would be desirable to increase the origin shift of block 2,3,4. However, the effect of such an increase on the peak field and on the field quality should also be taken into account:

- Block 2: an increase in origin shift allows to decrease the peak field in block 1 and to slightly improve the field quality.
- Block 3: the origin difference cannot be increased, because it would increase the peak field in block 1.
- Block 4: a small increase in origin shift improves the field quality and, to a small extent, the magnetic length, with no significant effect on the peak field. Larger increases are not allowed from the field quality standpoint (see REOPT1 case).

The origin differences which have been selected for each block are given in Table 5. The resulting geometry is shown in Fig. 7.

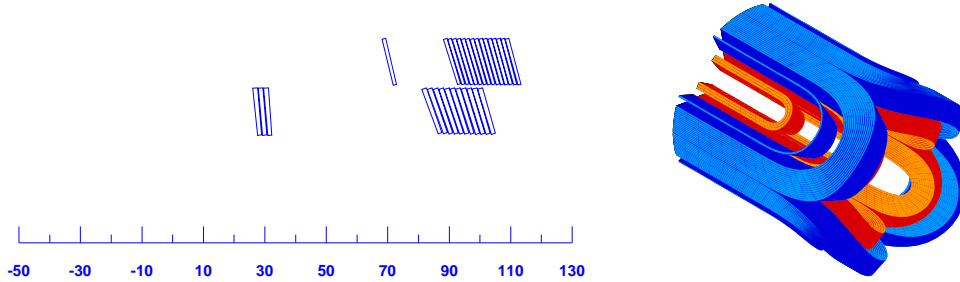


Figure 7: REOPT3 geometry. Axis scale for pole section is in mm.

Table 5: Origin differences (mm) for each conductor group in REOPT1-3, and corresponding values for HGQS02-3.

Group #	REOPT1	REOPT2	REOPT3	HGQS02-3
1	20	20	20	20
2	28	28	25	0
3 (A/B)	54	56/50	46	46
4	51	40	8	0

The magnetic analysis parameters for REOPT1-3 are given in Table 6. REOPT1 gives the largest increase in magnetic length (1.2 cm), but has a large negative dodecapole. Both REOPT2 and REOPT3 have very good field quality, and a reduced peak field with respect to the present configuration. In REOPT2, the magnetic length is increased by 7 mm, while in REOPT3 the gain is only 2 mm.

Table 6: Magnetic analysis parameters for REOPT1-3, and corresponding values for the return end configuration of HGQS02-3. L_p is the physical distance from the starting point $z_s=-10$ cm (5 cm before the iron yoke termination) to the outer edge of the outmost conductor group. L_m is the magnetic length from z_s to $+\infty$.

Parameter	Unit	REOPT1	REOPT2	REOPT3	HGQS02-3
L_p	cm	21.6	21.6	21.6	21.6
L_m	cm	18.7	18.2	17.7	17.5
$L_p - L_m$	cm	2.9	3.4	3.9	4.1
$B_{pk}^{(ic)}$	T/kA	0.68	0.66	0.64	0.65
$B_{pk}^{(oc)}$	T/kA	0.56	0.55	0.55	0.57
\hat{b}_6		-6.18	-0.05	0.10	2.3
\hat{b}_{10}		-0.15	-0.04	-0.32	-0.5
$\hat{b}_6 L_m$	m	-1.15	-0.01	0.02	0.4
$\hat{b}_{10} L_m$	m	-0.03	-0.01	-0.05	-0.09

7 Lead End Optimization

The lead end optimization assumes that an internal splice configuration will be adopted in HGQS05, and that the outer surface of the end plate will be located at $z=19$ cm (4 cm less than in HGQS03). The 2 cm origin shift of block 1 has been preserved in order to allow a wedge transition cut-out in the outer layer, although in the case of the lead end, where the transition between regular collars and end keys is at the beginning of the splice ramp, the motivation for introducing such a cut-out is not as strong as in the return end. The same magnetic analysis results would be obtained if the wedge transition cut-out would be eliminated and a negative shift of 2 cm would be applied to all blocks (including the splice ramps).

Since \hat{b}_6 is large and positive in HGQS03, it is possible to increase the magnetic length and at the same time improve the field quality without adding more spacers. A proposed optimized lead end geometry (LEOPT1) is shown in Fig. 8 (the corresponding origin differences are in Table 7).

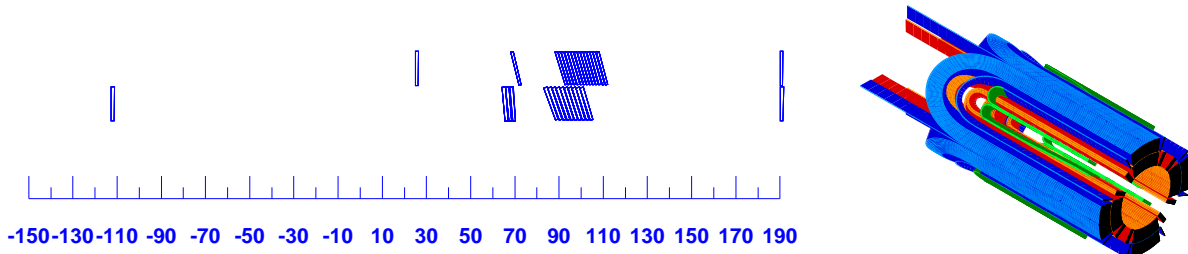


Figure 8: LEOPT1 geometry. The vertical bars indicate the end of the straight section for the splice conductors.

Table 7: Origin differences (mm) for each conductor group in LEOPT1, and corresponding values for HGQS03.

Group #	LEOPT1	HGQS03
1	20	20
2	25	0
3	48	46
4	46	0
Coil splice	20	0

Table 8: Magnetic analysis parameters for the optimized lead end configuration, and corresponding values for HGQS03. L_p is the physical distance from the starting point $z_s = -25$ cm (10 cm before the iron yoke termination) to the outer edge of the outmost conductor group. L_m is the magnetic length from z_s to $+\infty$.

Parameter	Unit	LEOPT1	HGQS03
L_p	cm	36.5	36.5
L_m	cm	32.3	31.5
$L_p - L_m$	cm	4.2	5.0
$B_{pk}^{(ic)}$	T/kA	0.64	0.64
$B_{pk}^{(oc)}$	T/kA	0.55	0.57
\hat{b}_6		1.04	6.57
\hat{b}_{10}		-0.13	-0.30
\hat{a}_2		54.0	57.7
\hat{a}_6		-1.06	-0.45
\hat{a}_{10}		-0.19	-0.05
$\hat{b}_6 L_m$	m	0.33	2.07
$\hat{b}_{10} L_m$	m	-0.04	-0.09
$\hat{a}_2 L_m$	m	17.5	18.2
$\hat{a}_6 L_m$	m	-0.33	-0.14
$\hat{a}_{10} L_m$	m	-0.06	-0.02

A comparison between the magnetic performance parameters of LEOPT1 and those of HGQS03 is given in Table 8. With the new configuration, the magnetic length is improved by 8 mm, and the peak field in the outer layer is decreased by 3%. As the normal dodecapole is reduced from 6 to 1 unit the skew dodecapole increases from -0.5 to -1 unit, thus setting a limit on the field quality optimization for this configuration. A second configuration (LEOPT2), where an additional spacer is introduced in the second-wound group of the inner layer, has been studied with the purpose of obtaining a further reduction of the field errors. However, the results up to this point have been inconclusive, and therefore are not reported here.

8 Conclusions

Several alternative optimized configurations for the lead and return ends of HGQS05 have been analyzed, and the most interesting cases have been presented, with the purpose of defining the design space for the magnetic performance parameters (magnetic length, peak field, field quality) and assessing relative advantages and costs of each solution. The final choice will depend on the relative weights placed on the different optimization objectives, which are not yet firmly defined at this stage. The proposed configurations should in any case be regarded as preliminary: a final magnetic optimization step will be necessary to improve the accuracy of the calculations (by using a refined model) and to include the results of the mechanical optimization still in progress (internal vs. external splice, end plate thickness, quadrant splice configuration).

References

- [1] A. Zlobin, “HGQ Short Model Program”, Fermilab TD-97-023, June 1997.
- [2] S. Caspi, “*LHC IR Quad*”, FNAL/LBL/CERN videoconference meeting, May 1st, 1996.
- [3] J. Brandt, A. Simmons, “Coil End Design for the LHC IR Quadrupole Magnet”, Fermilab TS-96-013, November 1996.
- [4] G. Sabbi, “Magnetic Field Analysis of HGQ Coil Ends”, Fermilab TD-97-040, September 1997.
- [5] G. Sabbi, J. Strait, A. Zlobin, S. Caspi, “Magnetic Field Analysis of the First Short Models of a High Gradient Quadrupole for the LHC Interaction Regions”, 15th International Conference on Magnet Technology, Beijing, China, October 1997.
- [6] G. Sabbi, “End Field Analysis of HGQ Model S02”, Fermilab TD-97-045, October 1997.
- [7] J. Brandt, “LHC IR Quad Internal Splice Design”, March 10, 1997.
- [8] G. Sabbi, “HGQS03 End Field Analysis”, Fermilab TD-98-010, February 5, 1998.
- [9] S. Russenschuck, “A computer program for the design of superconducting accelerator magnets”, Proc. ACES Symposium, Monterey, California, 1995 and CERN AT/95-39, September 1995.
- [10] G. Sabbi, “Comparison of Calculated vs. Measured Harmonics in HGQS01 Lead End”, Fermilab TD-98-036, May 1998.
- [11] G. Sabbi, “Load lines and short sample limits for HGQ model S01”, Fermilab TD-97-011, April 1997.
- [12] L. Walckiers, P. Lefevre, “Change of the reference radius for the LHC magnet”, LHC-MTA/LW, April 1998.